Reac Kinet Mech Cat (2018) 123:215–230
https://doi.org/10.1007/s11144-017-1286-8

Hydrogen atom transfer versus proton coupled electron transfer mechanism of gallic acid with different peroxy radicals

Dejan Milenković[1] · Jelena Đorović[1] · Vladimir Petrović[2] · Edina Avdović[2] · Zoran Marković[1,3]

Received: 19 August 2017 / Accepted: 27 September 2017 / Published online: 9 October 2017

Abstract Reactions of gallic acid (GA) with alkyl peroxy radicals (methylperoxy, ethylperoxy, *iso*-propylperoxy, and *tert*-butylperoxy) were simulated using density functional theory. The reaction is taking place in the way that hydrogen of hydroxy group of GA is transferred to the oxygen of each of peroxy radical. A newly formed radical is stabilized with delocalization of spin density over entire molecule, while the harmful peroxy radical is neutralized. These simple reactions can occur by two different, non-exclusive mechanisms: hydrogen atom transfer and proton coupled electron transfer. The competition between these mechanisms depends on both the solvent and the nature the free radicals. The main differences of these mechanisms are described, together with corresponding thermodynamic and kinetic consequences. The potency of this antioxidative action was thermodynamically and kinetically estimated for hydrogen atom transfer (HAT) and proton coupled electron transfer (PCET) mechanisms. The first one was estimated by calculating bond dissociation energy (ΔG_{BDE}), while the second one was examined using the activation barriers necessary for this action (transition state theory (TST)), as well as using the zero-curvature tunneling effect (ZCT). Additionally, the analysis of single occupied molecular orbitals (SOMOs) in transition states was used to examine differences between HAT and PCET mechanisms.

Electronic supplementary material The online version of this article (doi:10.1007/s11144-017-1286-8) contains supplementary material, which is available to authorized users.

✉ Zoran Marković
zmarkovic@np.ac.rs

[1] Bioengineering Research and Development Center, 34000 Kragujevac, Republic of Serbia

[2] Faculty of Science, University of Kragujevac, 12 Radoja Domanovića, 34000 Kragujevac, Republic of Serbia

[3] Department of Chemical-Technological Sciences, State University of Novi Pazar, Vuka Karadžića bb, 36300 Novi Pazar, Republic of Serbia

Keywords HAT · PCET · Gallic acid · Alkyl peroxy radicals

Introduction

The human body constantly generates free radicals and other reactive species. The state of cells in which the reactive radical species exceed the capacity of the endogenous antioxidative protection system is named oxidative stress [1, 2]. The oxidative degradation of the vital biomolecules, lipids, proteins, and nucleic acids is caused by processes which include the reactive free radical species, especially reactive oxygen species (ROS) [3, 4]. Biomolecules can be exposed to oxidative degradation for years, which promotes aging and increases risk for certain neurodegenerative diseases such as amyotrophic lateral sclerosis, Alzheimer's disease, and Parkinson's disease, and many other diseases [1, 4–8]. Modern studies indicate that oxidative stress can be decreased using antioxidants [9–11]. The consumption of fruits and vegetables has a preventive role, which is due to a variety of constituents, including minerals, vitamins, fiber, and numerous phytochemicals among which flavonoids and phenolic compounds are very important [12]. The possible association between the consumption of food containing phenolics and a reduced risk of developing several disorders, including cancer and cardiovascular diseases, has been evaluated in several epidemiological investigations [13–18]. Phenolic acids are rarely found as free molecules in nature, but they most commonly occur in plant materials as esters, amides, ethers, or as structural components of the cellulose, proteins, and lignin [19–21]. As everyday part of a human diet, they are involved in appreciation of good food quality, sensory qualities, color, nutritional, and antioxidant properties of foods. Especially, phenolic acids such as vanillic acid, 2,3-dihydroxybenzoic acid, 2,4-dihydroxybenzoic acid, and gallic acid (GA) have an important role. Their antioxidative efficiency has been related to the number of hydroxy groups in the molecule, and also to their hydrogen atom donating abilities [22].

GA can be found in gallnuts, witch hazel, tea leaves, oak bark, etc., as free and as a part of hydrolysable tannins [22–26]. GA is commonly used in pharmaceutical and chemical industry, as well as foodstuff. Besides being used as a standard for determination of the total phenol content in various analytes, it is also used as starting material in the organic synthesis. It also has great importance and application in medicine, acting as an antioxidant and helping in protection human cells against oxidative damage. It shows cytotoxicity against cancer cells, antiallergic, antitumor, antifungal, anti-inflammatory, antiseptic, antivirus and antiasthmatic effects. GA and its derivatives inhibit insulin degradation, and is particularly effective in treating albuminuria and diabetes, psoriasis and external hemorrhoids, coronary heart disease, cerebral thrombosis, gastric ulcer, snail fever, viral hepatitis, senile dementia and other diseases where oxidative stress is involved [27].

Antioxidant reactions of phenolic compounds take place in highly complex environments. This is a consequence of the presence of numerous different free radicals and antioxidants present in biological media. The concentrations and reactivity of mentioned species, as well as the polarity and the pH value of the environment have significant influence in these reactions. Therefore, in different media, various radicals can react via several mechanisms. The antiradical properties of antioxidants are based on their ability to donate hydrogen atom to a free radical. In these reactions, a newly formed radical is generated from the antioxidant molecule, and that newly formed species is more stable and less reactive than the initial free radical. There are numerous mechanisms of the antioxidant actions, and some of them are: hydrogen atom transfer (HAT), proton coupled electron transfer (PCET), single electron transfer followed by proton transfer (SET-PT), sequential proton loss electron transfer (SPLET), radical adduct formation (RAF), and sequential proton loss hydrogen atom transfer (SPLHAT) [28–32].

Understanding of the leading reaction mechanism involved in the antioxidant action is a challenging task. It is well known that reactions involving HAT mechanism between two oxygen atoms have much lower activation energies and higher rate constants than HAT mechanism between two carbon atoms [33]. HAT mechanism involves transfer of a proton with one of its bonding electrons. However, in the case of PCET mechanism, the proton is transferred from phenolic compound to the radical's lone pair. On the other hand, electron moves from the $2p$ lone pair of the phenol to the singly occupied molecular orbital (SOMO) of phenoxy radical [34, 35]. However, there are different approaches for determination which of these two mechanisms reaction obeys, including position of the orbitals between reacting species, tunneling effect, solvent polarity, etc. [36, 37].

In addition to our former thermodynamic investigation of antioxidative properties of GA, here we present a thermodynamic and mechanistic study of the reaction between the different peroxy radicals and GA. Since peroxy and methylperoxy (MP) radicals were used in our previous study [38–42], one of the aims of this work was to check the compatibility of thermodynamic and mechanistic approaches for antioxidative action of GA towards some alkyl peroxy radicals ($ROO^{\cdot}$). These radicals are soluble in membranes and considered to be the major generators of lipid peroxides [43]. They cause many kinds of diseases, including liver injury and cancer [44]. Akaike et al. found that $ROO^{\cdot}$ was generated by heme–iron-catalyzed decomposition of *t*-BuOOH, and that scavenging activity of various antioxidants towards these radicals can be estimated by electron spin resonance spectroscopy and chemiluminescence [45, 46]. Recently, it was shown that the *tert*-butylperoxy radical (tBP) has potent bactericidal action, and that the radical scavenging activity of various antioxidants can be quantitatively estimated on the basis of the inhibitory activity against the $ROO^{\cdot}$ induced cytotoxicity toward *Staphylococcus aureus* [45, 47]. However, there are no reports on the estimation of the free scavenging activity of gallic acid against $ROO^{\cdot}$.

Methodology

Geometry optimizations for all participants under investigation and frequency calculations have been carried out using a M05-2X method [48] combined with the 6-311++G(d,p) basis set. To account for the solvent effects, two solvents were investigated (water and benzene) using SMD model as implemented in Gaussian 09 [49, 50]. All geometries were fully optimized without imposing any restriction. The nature of the revealed stationary points on potential energy surface was confirmed by analyzing the results of the frequency calculations: no imaginary frequencies for equilibrium geometries, and one imaginary frequency for transition states.

In the case of the transition states, it was verified that the imaginary frequency corresponds to the expected motion along the reaction coordinate by intrinsic coordinate calculations (IRC). These calculations proved that each transition state (TS) connects two corresponding energy minima: reactant complex (RC) and product complex (PC). Natural bond orbital (NBO) analysis was performed for all participants in simulated reaction of the $ROO^{\cdot}$ and GA [51, 52].

Transition state theory (TST) affords one of the simplest theoretical approaches for estimating the rate constants (k), which requires only structural, energetic, and vibrational frequency information for reactants and transition states [53]. The main advantage of using conventional TST is that it requires very limited potential energy information (only on reactants and the transition state), which makes it practical for a wide range of chemical reactions. Despite its relative simplicity, this theory has been proven to be sufficient to reproduce experimental rate constants of free radical scavenging reactions [54].

The rate constants for the reactions of $CR_3OO^{\cdot}$ and GA were calculated using TST, implemented in TheRate program [55] and 1 M standard state is calculated as follows:

$$k^{TST} = \frac{k_B T}{h} \exp\left(\frac{-\Delta G^{\neq}}{RT}\right). \tag{1}$$

Here k_B and h stand for the Boltzmann and Planck constants, $\Delta G^{\neq}$ is the free energy of activation, which is calculated as the difference in energies between transition states and reactants. In the case of HAT/PCET mechanism, reaction path degeneracy (σ) and transmission coefficient $\gamma(T)$ were taken into account, implying that the Eyring equation was transformed into:

$$k^{ZCT} = \sigma\gamma(T) \frac{k_B T}{h} \exp\left(\frac{-\Delta G^{\neq}}{RT}\right). \tag{2}$$

The transmission coefficient γ, corrections for tunneling effects (defined as the Boltzmann average of the ratio between the quantum and classical probabilities), was calculated using the zero-curvature tunneling (ZCT) approach [56].

Results and discussion

In our previous work, we investigated thermodynamic properties of the reactions of GA with $^{\cdot}OH$, $^{\cdot}\overline{\ }O_2$, and $^{\cdot}OOCH_3$ radicals [38]. It was found that position 4 is the most reactive site of GA, while positions 3 and 5 are mutually identical. In extension, here we examine reactions of GA with $ROO^{\cdot}$ such as: methylperoxy (MP), ethylperoxy (EP), *iso*-propylperoxy (iPP) and *tert*-butylperoxy (tBP) radicals (Scheme 1), by applying the kinetic approach. The atom labeling presented in Scheme 1 is used through the whole manuscript. In all investigated cases, the transfer of hydrogen atom/proton is the process of interest. This transition is taking place from hydroxy group of GA to the oxygen of each of corresponding radicals. In this way, reactive peroxy radicals are neutralized, and new, more stable radical products are formed from GA. The rate constants k^{TST} and k^{ZCT} for all reaction of peroxy radicals and GA were calculated using Eqs. 1 and 2. The bond dissociation energies (ΔG_{BDE}) as well as the activation energies and the rate constants at 298 K are presented in Tables 1 and 2.

Hydrogen atom transfer-thermodynamics

Among the three hydroxy groups of GA, 4-OH group is the most responsible for the antiradical activity [38–42]. It is well known that $\Delta \boldsymbol{G}_{BDE}$ for the HAT mechanism can be calculated using the following equation:

$$\Delta \boldsymbol{G}_{BDE} = \boldsymbol{G}(\mathrm{GA{-}O^{\cdot}}) + \mathrm{G}(\mathrm{CR_3OOH}) - \boldsymbol{G}(\mathrm{GA{-}OH}) - \boldsymbol{G}(\mathrm{CR_3OO^{\cdot}})$$

Here $\boldsymbol{G}$(GA–O$^{\cdot}$), $\boldsymbol{G}$(CR_3OOH), $\boldsymbol{G}$(GA–OH), and $\boldsymbol{G}$($CR_3OO^{\cdot}$) are the free energies of the gallic acid radical, molecule formed when corresponding peroxy radical accepts hydrogen atom from the gallic acid, gallic acid, and different free radical species, respectively. Lower values of $\Delta \boldsymbol{G}_{BDE}$ mean higher ability of GA to donate a hydrogen atom to corresponding radical species.

The results with all free radicals indicate that all reactions with *p*-OH group of GA both in water and benzene are exergonic. As regards, H transfer from *m*-OH of GA all reactions are endergonic in both solvents, except for the case of MP radical

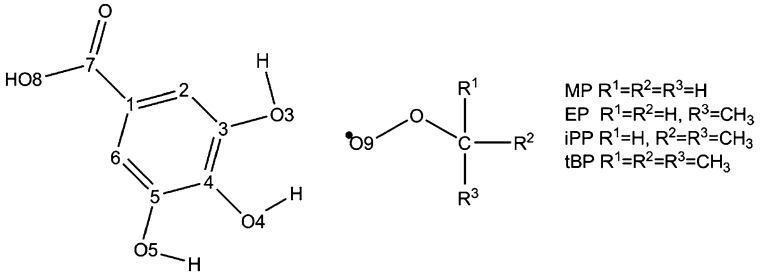

$$\mathrm{GA{-}OH + CR_3OO^{\bullet} \rightarrow GA{-}O^{\bullet} + CR_3OOH}$$

Scheme 1 Atomic numbering of gallic acid and examined alkyl peroxy radicals

Table 1 The calculated ΔG_{BDE} (kJ/mol) for the reactions of GA with alkyl peroxy radicals

	Water ΔG_{BDE}	Benzene ΔG_{BDE}
GAOH-3 + MP	− 0.61	4.11
GAOH-3 + EP	1.02	5.66
GAOH-3 + iPP	3.43	7.90
GAOH-3 + tBP	4.98	10.3
GAOH-4 + MP	− 18.5	− 20.4
GAOH-4 + EP	− 16.8	− 18.8
GAOH-4 + iPP	− 14.4	− 16.6
GAOH-4 + tBP	− 12.8	− 14.2

(Table 1). This indicates that the HAT reaction mechanism of GA with all $ROO^{\cdot}$ is thermodynamically possible for *p*-OH group of GA in both solvents, while this mechanism is not preferable for *m*-OH. These results are in accordance with the results of previous investigation [38, 57].

To explain the differences in the reactivity of the individual OH sites the assessment of the spin density distribution was undertaken on the radicals of GA (positions 3 and 4). The lower ΔG_{BDE} values implicate easier formation of the radicals and more delocalized spin density. The spin density values in water, obtained by the NBO analysis, as well as SOMOs of GA are depicted in Figs. 1 and S1. The results show that the radical formed from GA in position 4 is more stable. This is consequence of delocalization of the unpaired electron over oxygen and *ortho* and *para* carbons of aromatic core of GA (Fig. 1). In addition, appearance of low values of spin density in the GA–$4O^{\cdot}$ on the two adjacent OH groups, as well as carboxyl group, suggests that unpaired electron is additionally delocalized, explaining higher stability compared to GA–$3O^{\cdot}$.

Kinetics of HAT and PCET mechanism

There are several approaches examining g differences between HAT and PCET mechanisms, including different positioning of the reacting species and different electronic characters [58]. In this study, we considered differences between HAT and PCET mechanisms examining geometry orientations of all alkyl peroxy radicals toward GA in transition states as given. Potential energy surfaces and the optimized structures of stationary points along reaction pathways of HAT mechanism in water, and PCET mechanism in benzene are presented in Fig. 2, while the optimized structures of all other transition states are provided in Figs. S2 and S3.

It was found that the barrier is slightly higher in benzene than in polar media for reaction of MP with 3-OH group, while in the case of EP, iPP, tBP the barriers are slightly lower in benzene (Table 2). Comparing the reactivity of the GA (both 3 and 4 positions in both solvents), it was found that the energy barrier for H transfer from phenolic site 4 is significantly lower than for 3. The difference is about 20 kJ/mol in the case of HAT and about 10 kJ/mol for PCET. The obtained results strongly suggest a higher reactivity of the *para* hydroxy group.

Table 2 The calculated values of kinetic parameters for the reaction of GA and free peroxy radicals. $\Delta G^{\neq}$, k^{TST}, k^{ZCT}, γ and ΔG_r denote activation free energy, rate constants, transmission coefficient ($\gamma = k^{ZCT}/k^{TST}$) and reaction free energy, respectively

	HAT				PCET			
	$\Delta G^{\neq}$ (kJ/mol)	k^{TST} (M^{-1} s^{-1})	k^{ZCT} (M^{-1} s^{-1})	γ	$\Delta G^{\neq}$ (kJ/mol)	k^{TST} (M^{-1} s^{-1})	k^{ZCT} (M^{-1} s^{-1})	γ
Water								
GA–3O˙								
MP	54.4	1.83×10^{3}	2.32×10^{6}	1.27×10^{3}	–	–	–	–
EP	63.3	5.01×10^{1}	1.05×10^{5}	2.10×10^{3}	–	–	–	–
iPP	65.8	1.86×10^{1}	4.07×10^{5}	2.19×10^{4}	–	–	–	–
tBP	69.3	4.00×10^{0}	9.28×10^{5}	2.04×10^{4}	–	–	–	–
GA–4O˙								
MP	33.4	8.59×10^{6}	8.54×10^{8}	9.96×10^{1}	–	–	–	–
EP	34.0	6.82×10^{6}	8.19×10^{8}	1.20×10^{2}	–	–	–	–
iPP	36.9	2.16×10^{6}	6.49×10^{8}	3.00×10^{2}	–	–	–	–
tBP	39.8	6.51×10^{5}	1.23×10^{9}	1.89×10^{3}	–	–	–	–
Benzene								
GA–3O˙								
MP	59.9	1.97×10^{2}	1.15×10^{5}	5.82×10^{2}	73.1	9.75×10^{-1}	1.69×10^{4}	5.67×10^{4}
EP	61.2	1.16×10^{2}	8.29×10^{4}	7.12×10^{2}	74.7	5.00×10^{-1}	7.17×10^{4}	6.19×10^{4}
iPP	62.3	7.63×10^{1}	5.94×10^{4}	7.78×10^{2}	75.8	3.28×10^{-1}	2.09×10^{4}	6.37×10^{4}
tBP	62.7	6.37×10^{1}	1.31×10^{5}	2.06×10^{3}	76.0	3.06×10^{-1}	1.33×10^{4}	4.34×10^{4}
GA–4O˙								
MP	39.7	6.79×10^{5}	5.17×10^{7}	7.61×10^{1}	63.9	3.99×10^{1}	2.20×10^{6}	5.51×10^{4}
EP	40.7	4.59×10^{5}	4.71×10^{7}	1.03×10^{2}	64.4	2.36×10^{1}	1.83×10^{6}	5.62×10^{4}
iPP	40.6	4.70×10^{5}	6.33×10^{7}	1.35×10^{2}	65.8	1.82×10^{1}	1.16×10^{6}	6.38×10^{4}
tBP	41.3	3.59×10^{5}	1.84×10^{8}	5.11×10^{2}	65.6	2.02×10^{1}	2.02×10^{6}	9.99×10^{4}

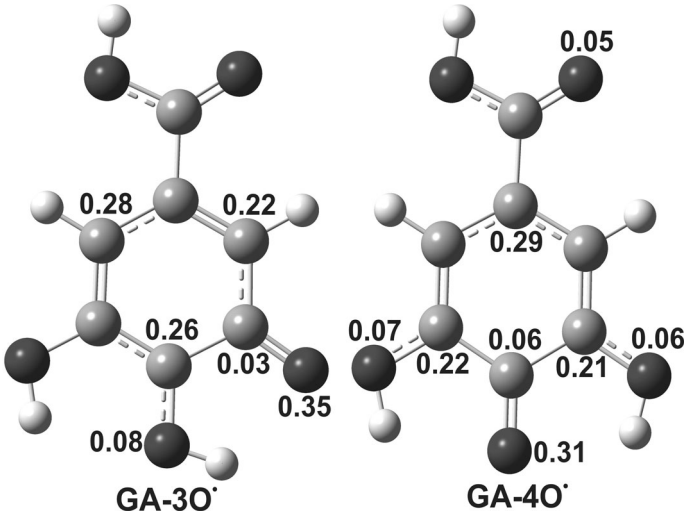

Fig. 1 Spin density distribution in GA radicals in water

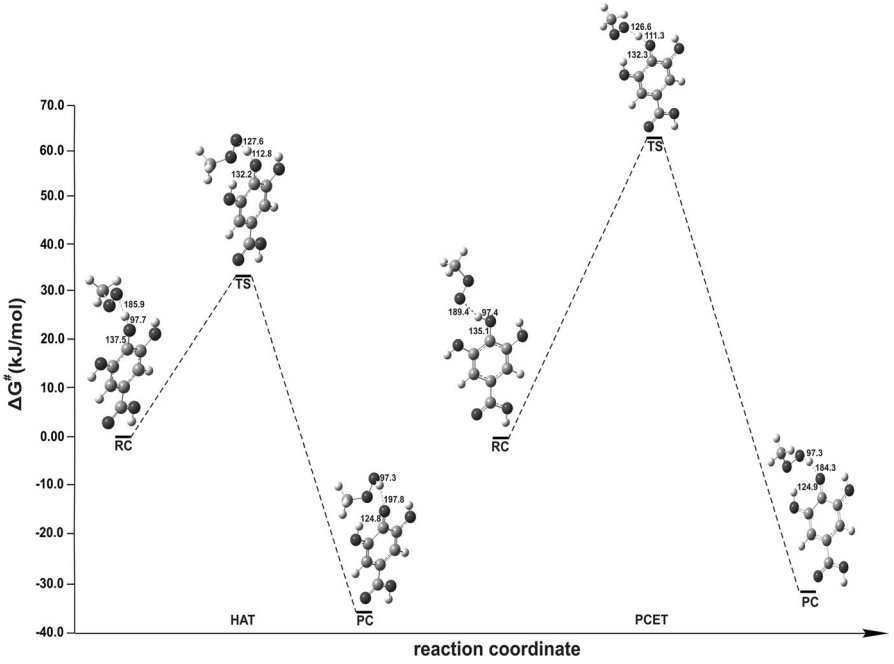

Fig. 2 Reaction pathway for the H-atom transfer from the C4–OH position of GA to the MP radical, in water (HAT) and benzene (PCET). The distances between C=O, O–H and H–O9 bonds are given in pm

On the basis of the obtained results from Table 2, it is evident that Gibbs activation energies and rate constants for HAT mechanisms are not heavily influenced by the solvent polarity. In addition, we were not able to locate transition states responsible for PCET mechanism in water, as polar solvent. As a consequence of the previously mentioned lower activation barriers for position 4, k^{TST} values are larger in comparison to those in position 3, implying that reaction in position 4 is significantly faster. Studies of kinetic solvent effects (KSEs) for the reaction in water and for related reaction in benzene, demonstrated that HAT in water and benzene exhibited gentle influence of KSEs, for example for MP $k^{TST} = 8.59 \times 10^5$ in water, while $k^{TST} = 6.79 \times 10^5$ in benzene. It means that the reactions which are taking place via the HAT mechanism are somewhat slower in a non-polar solvent. Similarly to the case of HAT, position 4 of GA is more reactive via PCET mechanism (Table 2). In contrast to the HAT mechanism, here the KSEs play an important role, since the reaction by PCET mechanism takes place only in the non-polar solvent (Table 2). The influence of the branched alkyl group of investigated peroxy radicals on the rate of chemical reaction showed that there is a slight decrease in the rate of the reaction with increase in the branching of alkyl group, in the case of both mechanisms.

Insight into k^{ZCT} and γ points out tunneling effects as the responsible one for making the reaction between GA and alkyl peroxy radicals faster, in both positions and in both solvents (Table 2). Namely, values for MP radical reaction in position 4 of $k^{ZCT} = 8.54 \times 10^8$ in water, and $k^{zct} = 5.17 \times 10^7$ in benzene clearly show that tunneling effect is playing very important role. It is worth pointing out that the tunneling effect is responsible for the increase in reactions rate constants in all positions, and all solvents (Table 2; Figs. 3, S4 and S5). This effect rapidly decreases with the increase in the temperature. Since the abstraction reaction involves the motion of a light particle (hydrogen atom) that can easily tunnel

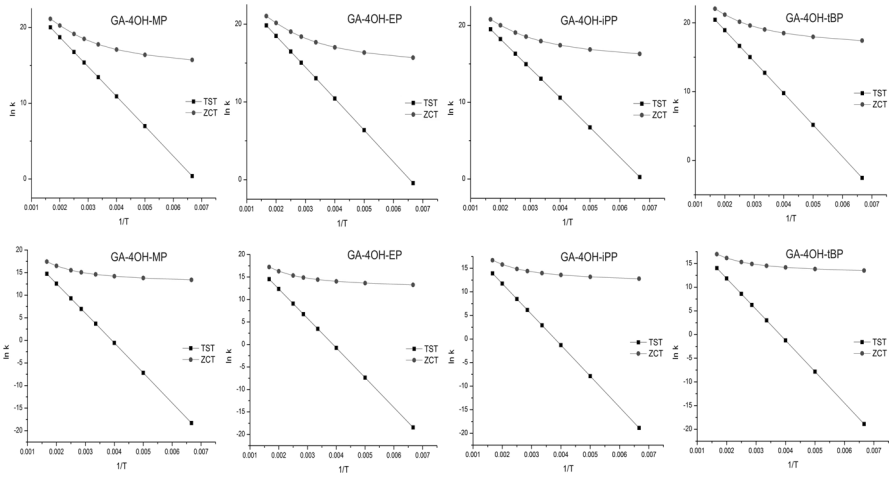

Fig. 3 Dependence of $\ln k^{TST}$ and $\ln k^{ZCT}$ (M^{-1} s^{-1}) on reciprocal temperature 1/T (K) in the HAT (top) and PCET (bottom) pathways of GA with alkyl peroxy radicals, in benzene

through the reaction barrier, this action is to be expected (reaction of "pure" HAT mechanism). In addition, the reactions in position 4 of GA are distinctly exergonic (Table 2), while the activation energies are low and corresponding rate constants high. As in the case of the HAT reactions for the trapping of peroxy radicals by GA, reactions in positions 3 and 4 of PCET reaction in benzene have pronounced tunneling effect, too. In addition, transmission coefficients (γ) are obviously much higher in the case of PCET, implying different pathways for proton and electron motion [58]. The tunneling effect can be attributed to the formation of a compact H-bonded complex via two H bonds between the donor and acceptor and the short path length for hydrogen transfer indicating that the H transfer proceeds via a PCET mechanism [58–60]. Nevertheless, although tunneling effect is more pronounced in the case of PCET mechanism, the values for k^{ZCT} show the same trends as k^{TST} values, and point out HAT as preferable reaction pathway. It is worth pointing out that with the increase in branching of alkyl group of radical, i.e. increase in electron donating ability of alkyl moiety, the tunneling effect is becoming more pronounced.

All these facts suggest that the reaction pathway of HAT mechanism in position 4 is predominant in both solvents [61]. Therefore, this process exposes the highest rate constant values, which can be attributed to the involvement of O4 from gallic acid radical in the relatively strong hydrogen bonds with H3 and H5, contributing to the weakening of the O4–H4 bond. The reaction of MP is slightly favored, by both thermodynamic and kinetic parameters. Inspection of the rate constant values in benzene for PCET mechanism indicated that, again, position 4 is also more probable reacting site. However, if one compares these parameters with those obtained for HAT, it is obvious that HAT is more probable mechanism.

Taking into account pK_a value of carboxylate group of GA (4.4) [62], and that GA is deprotonated in aqueous solution (87.3%) [57, 63], it means the carboxylate anion of GA might play an important role is antioxidative action under physiological conditions (pH 7.4). Therefore, radical scavenging action of GA carboxylate anion against all investigated peroxy radicals has been investigated (Table S2). Based on the obtained values of activation energies, it is clear that corresponding reaction with all investigated radicals are slightly faster than those with GA itself.

HAT versus PCET

The values of the partial negative charge and the spin density in benzene, obtained by NBO analysis, on corresponding oxygen atoms for the RCs, TSs, and PCs are presented in the Table 3. On the basis of the obtained results, one can see that during the reaction the partial negative charge on peroxy O9 increases, and has the highest value in PCs. In the contrast to this, the partial negative charge on the phenolic oxygen O4 decreases in all cases. The partial positive charges on phenolic hydrogens are around 0.5, with small variations during the reactions. On the other hand, the spin density value on O9 is about 0.7 in all RCs, while the spin density values on all other atoms are practically equal to zero. The spin density is shared between O9 and the phenolic oxygen O4 in TSs (Table 3). Finally, in all PCs, the spin density is distributed over the GA moiety, while its value on O9 is decreased to

Table 3 Partial charge and spin density values of the oxygen atoms of interest in benzene

	Atom	HAT						PCET					
		Partial charge			Spin density			Partial charge			Spin density		
		RC	TS	PC	RC	TS	PC	RC	TS	PC	RC	TS	PC
MP	O4	− 0.74	− 0.72	− 0.65	0.00	0.15	0.31	− 0.74	− 0.69	− 0.66	0.00	0.18	0.30
	O9	− 0.20	− 0.37	− 0.50	0.67	0.31	0.00	− 0.20	− 0.34	− 0.46	0.67	0.37	0.00
EP	O4	− 0.74	− 0.72	− 0.66	0.00	0.15	0.29	− 0.74	− 0.69	− 0.66	0.00	0.19	0.31
	O9	− 0.21	− 0.38	− 0.48	0.67	0.31	0.00	− 0.20	− 0.35	− 0.47	0.67	0.36	0.00
iPP	O4	− 0.74	− 0.71	− 0.66	0.00	0.17	0.31	− 0.74	− 0.69	− 0.66	0.00	0.19	0.31
	O9	− 0.20	− 0.38	− 0.47	0.67	0.31	0.00	− 0.20	− 0.35	− 0.47	0.67	0.36	0.00
tBP	O4	− 0.74	− 0.72	− 0.65	0.00	0.16	0.31	− 0.74	− 0.69	− 0.65	0.00	0.19	0.31
	O9	− 0.21	− 0.38	− 0.47	0.66	0.30	0.00	− 0.21	− 0.35	− 0.47	0.66	0.36	0.00

zero. This finding confirms that every PC consists of alkyl peroxide and the corresponding GA–4O$^{\cdot}$ species. Spin delocalization in this product is in agreement with the fact that more stable radical is formed. During all reaction pathways, the spin density on the phenolic hydrogens (H4) remains close to zero. All these facts indicate that the spin density on the transferred hydrogen cannot be generally used to distinguish HAT from PCET mechanism [35], but some other results point out differences between PCET and HAT mechanism.

Mayer et al. used DFT to examine the self-exchange reactions of the phenoxy radical/phenol, methoxy radical/methanol and the benzyl radical/toluene systems [64]. They identified the geometrical differences of HAT and PCET in transitions states. The identification was based on the analysis of the SOMO of the transition state. The HAT mechanism is characterized by a significant SOMO density along the donor ···H··· acceptor transition vector. On the other hand, SOMO of PCET transition state involves *p* type orbitals, which are orthogonal to the transition vector.

The analysis of SOMOs shapes in the corresponding HAT and PCET transition states provides deeper insight into the differences between these mechanisms (Fig. 4). SOMOs of all TSs of HAT and PCET are mostly localized over aromatic ring of GA. On the other hand, differences are obvious along the O4···H4···O9 vectors. Namely, in all HAT transition states, SOMOs are also localized along this transition vector, implying that the transfer of hydrogen atom is taking place. On the

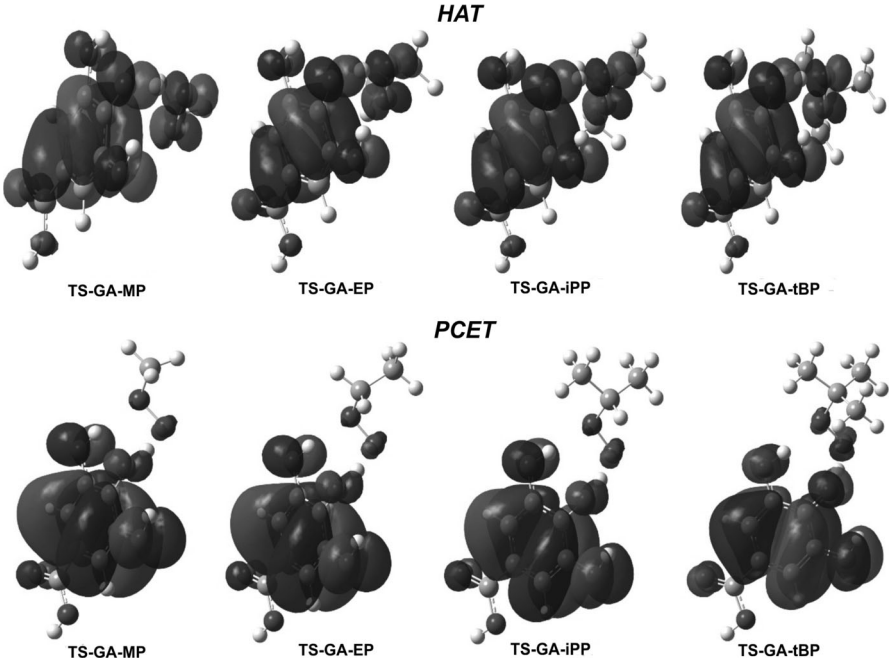

Fig. 4 The shape of SOMOs in different transition states of HAT and PCET mechanisms in position 4, in benzene

other hand, the SOMOs of PCET in TSs involve the *p* orbitals in the H acceptor (O4), and they are not localized along O4···H4···O9 transition vector. Here, the transfer of a proton and electron follows different pathways, indicating that the proton is transferred from the OH group in position 4 of GA to oxygen's lone pair of radical, while the electron moves from the 2*p* lone pair of the GA–4OH to the SOMO of alkyl peroxy radical. These findings are in good agreement with literature data [65].

Additionally, delocalization of SOMO is significantly weaker in transition states of PCET than in those for HAT mechanism. These differences rationalize the higher activation energies for the reactions via PCET mechanism (Table 2). Namely, PCET is energetically disfavored for about 24 kJ/mol in all cases.

Conclusion

In this paper, we presented thermodynamic and kinetic approach for the antioxidative action of gallic acid with some alkyl peroxy radicals, via HAT and PCET mechanisms, in polar and non-polar solvents. Based on the obtained results, it can be concluded that PCET mechanism is not possible in water for the examined system. Furthermore, ΔG_{BDE} as well as k^{TST} rate constants are undoubtedly showing that HAT is predominant mechanism in both solvents. Thermodynamic and kinetic data clearly point out position 4 as more reactive site of the GA. In addition, the large tunneling effect is sharpening the potential barriers for both mechanisms. Moreover, the obtained k^{ZCT} values are in agreement with those for k^{TST} also implying that HAT is prevailing mechanism. Furthermore, it is shown that differences between HAT and PCET mechanisms cannot be distinguished using NBO charges and spin densities. Instead, for this purpose, SOMOs are used to interpret these differences. The obtained results showed that, unlike HAT TSs structures, there is no SOMO localization over O4···H4···O9 transition vector in PCET transition states. Consequently, HAT activation barriers are favored by about 24 kJ/mol, in all cases. This additionally points out HAT as preferred mechanistic pathway under examined reaction conditions.

Acknowledgements The authors gratefully acknowledge financial support from the Ministry of Science of Republic of Serbia (Project Nos. 172015, 174028, and 172016).

Compliance with ethical standards

Conflict of interest The authors declare that there is no conflict of interests regarding the publication of this paper.

References

1. Barnham KJ, Masters CL, Bush AI (2004) Neurodegenerative diseases and oxidative stress. Nat Rev Drug Discov 3:205–214

2. Sayre LM, Perry G, Smith MA (2008) Oxidative stress and neurotoxicity. Chem Res Toxicol 21:172–188
3. Barber SC, Mead RJ, Shaw PJ (2006) Oxidative stress in ALS: a mechanism of neurodegeneration and a therapeutic target. Biochim Biophys Acta Mol Basis Dis 1762:1051–1067
4. Ames BN, Shigenaga MK, Hagen TM (1993) Oxidants, antioxidants, and the degenerative diseases of aging. Proc Natl Acad Sci USA 90:7915–7922
5. Halliwell B, Gutteridge JMC (1999) Free Radicals in Biology and Medicine, 3rd edn. Clarendon Press, Oxford
6. Sies H (ed) (1991) Oxidative stress, oxidants and antioxidants. Academic Press, New York
7. Thomas CE, Kalyanaraman B (1998) Oxygen radicals and the disease process. Harwood Academic Publishers, London
8. Halliwel B (2001) Free radicals and other reactive species in disease. Nature Publishing Group, London
9. Lleó A, Greenberg SM, Growdon JH (2006) Current pharmacotherapy for Alzheimer's disease. Annu Rev Med 57:513–533
10. Moosmann B, Behl C (2002) Antioxidants as treatment for neurodegenerative disorders. Expert Opin Investig Drugs 11:1407–1435
11. Troadec JD, Marien M, Darios F, Hartmann A, Ruberg M, Colpaert F, Michel PP (2008) Noradrenaline provides long-term protection to dopaminergic neurons by reducing oxidative stress. J Neurochem 7:200–210
12. Tomás-Barberán FA, Espin JC (2001) Phenolic compounds and related enzymes as determinants of quality in fruits and vegetables. J Sci Food Agric 81:853–876
13. You BR, Kim SZ, Kim SH, Park WH (2011) Gallic acid-induced lung cancer cell death is accompanied by ROS increase and glutathione depletion. Mol Cell Biochem 357:295–303
14. You BR, Moon HJ, Han YH, Park WH (2010) Gallic acid inhibits the growth of HeLa cervical cancer cells via apoptosis and/or necrosis. Food Chem Toxicol 48:1334–1340
15. Elango S, Balwas R, Padma VV (2011) Gallic acid isolated from pomegranate peel extract induces reactive oxygen species mediated apoptosis in A549 cell line. J Cancer Ther 2:638–645
16. Lecumberri E, Dupertuis YM, Miralbell R, Pichard C (2013) Green tea polyphenol epigallocatechin-3-gallate (EGCG) as adjuvant in cancer therapy. Clin Nutr 32:894–903
17. Saxena HO, Faridi U, Srivastava S, Kumar JK, Darokar MP, Luqman S, Chanotiya CS, Krishna V, Negi AS, Khanuja SPS (2008) Gallic acid-based indanone derivatives as anticancer agents. Bioorg Med Chem Lett 18:3914–3918
18. Zeng L, Holly JM, Perks CM (2014) Effects of physiological levels of the green tea extract epigallocatechin-3-gallate on breast cancer cells. Front Endocrinol (Lausanne) 5:61
19. Andreasen MF, Christensen LP, Meyer AS, Hansen A (2000) Content of phenolic acids and ferulic acid dehydrodimers in 17 rye (*Secale cereale* L.) varieties. J Agric Food Chem 48:2837–2842
20. Lam TBT, Kadoya K, Iiyama K (2001) Bonding of hydroxycinnamic acids to lignin: ferulic and p-coumaric acids are predominantly linked at the benzyl position of lignin, not the â-position, in grass cell walls. Phytochemistry 57:987–992
21. Brett C, Waldron K (1996) Cell wall architecture and the skeletal role of the cell wall. In: Brett C, Waldron K (eds) Physiology and biochemistry of plant cell walls. Chapman and Hall, London
22. Bianco MA, Handaji A, Savolainen H (1998) Quantitative analysis of ellagic acid in hardwood samples. Sci Total Environ 222:123–126
23. Pettersen RC, Ward JC, Lawrence AH (1993) Detection of northern red oak wetwood by fast heating and ion mobility spectrometric analysis. Holzforschung 47:513–522
24. Koga T, Moro K, Nakamori K, Yamakoshi J, Hosoyama H, Kataoka S, Ariga T (1999) Increase of antioxidative potential of rat plasma by oral administration of proanthocyanidin-rich extract from grape seeds. J Agric Food Chem 47:1892–1897
25. Burns J, Gardner PT, O'Neil J, Crawford S, Morecroft I, McPhail DB, Lister C, Matthews D, MacLean MR, Lean MEJ, Duthie GG, Crozier A (2000) Relantionship among antioxidant activity, vasodilation capacity, and phenolic content of red wines. J Agric Food Chem 48:220–230
26. Sakagami H, Yokote Y, Akahane K (2001) Changes in amino acid pool and utilization during apoptosis in HL-60 cells induced by epigallocatechin gallate or gallic acid. Anticancer Res 21:2441–2447
27. Gutteridge JMC, Halliwell B (1994) Antioxidants in nutrition, health, and disease, 1st edn. Oxford University Press, Oxford

28. Klein E, Lukeš V, Ilèin M (2007) DFT/B3LYP study of tocopherols and chromans antioxidant action energetics. Chem Phys 336:51–57
29. Litwinienko G, Ingold KU (2007) Solvent effects on the rates and mechanisms of reaction of phenols with free radicals. Acc Chem Res 40:222–230
30. Galano A (2015) Free radicals induced oxidative stress at a molecular level: the current status, challenges and perspectives of computational chemistry based protocols. J Mex Chem Soc 59:231–262
31. Galano A, Mazzone G, Alvarez DR, Marino T, Alvarez- Idaboy JR, Russo N (2016) Food antioxidants: chemical insights at the molecular level. Ann Rev Food Sci T 7:335–352
32. Mazzone G, Galano A, Alvarez-Idaboy JR, Russo N (2016) Coumarin-chalcone hybrids as peroxyl radical scavengers: kinetics and mechanisms. J Chem In Model 56:662–670
33. Min DB, Boff JM (2002) Chemistry and reaction of singlet oxygen in foods. Compr Rev Food Sci Food Saf 1:58–72
34. Rose RC, Bode AM (1993) Biology of free radical scavengers: an evaluation of ascorbate. FASEB J 7:1135–1142
35. Mayer JM (2004) Proton-coupled electron transfer: a reaction chemist's view. Ann Rev Phys Chem 55:363–390
36. Skone JH, Soudackov AV, Hammes-Schiffer SJ (2006) Calculation of vibronic couplings for phenoxyl/phenol and benzyl/toluene self-exchange reactions: implications for proton-coupled electron transfer mechanisms. J Am Chem Soc 128:16655–16663
37. Tishchenko O, Truhlar DG, Ceulemans A, Nguyen MTJ (2008) A unified perspective on the hydrogen atom transfer and proton-coupled electron transfer mechanisms in terms of topographic features of the ground and excited potential energy surfaces as exemplified by the reaction between phenol and radicals. J Am Chem Soc 130:7000–7010
38. Đorović J, Marković JMD, Stepanić V, Begović N, Amiæ D, Marković Z (2014) Influence of different free radicals on scavenging potency of gallic acid. J Mol Model 20:2345
39. Chen Y, Xiao H, Zheng J, Liang G (2015) Structure–thermodynamics–antioxidant activity relationships of selected natural phenolic acids and derivatives: an experimental and theoretical evaluation. PLoS ONE 10:e0121276
40. Koroleva O, Torkova A, Nikolaev I, Khrameeva E, Fedorova T, Tsentalovich M, Amarowicz R (2014) Evaluation of the antiradical properties of phenolic acids. Int J Mol Sci 15(9):16351–16380
41. Leopoldini M, Marino T, Russo N, Toscano M (2004) Antioxidant properties of phenolic compounds: H-atom versus electron transfer mechanism. J Phys Chem A 108(22):4916–4922
42. Saqib M, Mahmood A, Akram R, Khalid B, Afzal S, Kamal GM (2015) Density functional theory for exploring the structural characteristics and their effects on the antioxidant properties. J Pharm Appl Chem 1(2):65–71
43. Watabe T, Tsubaki A, Isobe M, Ozawa N, Hiratsuka A (1984) A mechanism for epoxidation of cholesterol by hepatic microsomal lipid hydroperoxides. Biochim Biophys Acta 795:60–66
44. Fraga CG, Tappel AL (1988) Damage to DNA concurrent with lipid peroxidation in rat liver slices. Biochem J 252:893–896
45. Akaike T, Sato KIS, Miyamoto YK, Ando MM, Maeda H (1992) Bactericidal activity of alkyl peroxyl radicals generated by heme-iron-catalyzed decomposition of organic peroxides. Arch Biochem Biophys 294:55–63
46. Maeda H, Katsuki T, Akaike T, Yasutake R (1992) High correlation between lipid peroxide radical and tumor-promoter effect: suppression of tumor promotion in the Epstein-Barr virus/B-lymphocyte system and scavenging of alkyl peroxide radicals by various vegetable extracts. Jpn J Cancer Res 83:923–928
47. Akaike T, Ijiri S, Sato K, Katsuki T, Maeda H (1995) Determination of peroxyl radical-scavenging activity in food by using bactericidal action of alkyl peroxyl radical. J Agric Food Chem 43:1864–1870
48. Zhao Y, Schultz NE, Truhlar DG (2006) Design of density functionals by combining the method of constraint satisfaction with parametrization for thermochemistry, thermochemical kinetics, and noncovalent interactions. J Chem Theo Comp 2:364–382
49. Frisch MJ, Trucks GW, Schlegel HB, Scuseria GE, Robb MA, Cheeseman G, Scalmani JR, Barone V, Mennucci B, Petersson H, Nakatsuji GA, Caricato HP, Li MX, Hratchian HP, Izmaylov AF, Bloino JL, Zheng J, Sonnenberg G, Hada M, Ehara M, Toyota K, Fukuda R, Hasegawa J, Ishida M, Nakajima T, Honda Y, Kitao O, Nakai H, Vreven T, Montgomery JE, Peralta JA, Ogliaro F, Bearpark M, Heyd JJ, Brothers E, Kudin KN, Staroverov R, Kobayashi VN, Normand K, Raghavachari J,

Rendell A, Burant JC, Iyengar SS, Tomasi J, Cossi M, Rega NJ, Millam M, Klene M, Knox JE, Cross JB, Bakken V, Adamo C, Jaramillo J, Gomperts R, Stratmann RE, Yazyev O, Austin AJ, Cammi R, Pomelli C, Ochterski JW, Martin RL, Morokuma K, Zakrzewski VG, Voth GA, Salvador P, Dannenberg S, Dapprich JJ, Daniels AD, Farkas Ö, Foresman JB, Ortiz JV, Cioslowski J, Fox DJ (2009) Gaussian 09, Revision C.01. Gaussian Inc, Wallingford

50. Marenich AV, Cramer CJ, Truhlar DG (2009) Performance of SM6, SM8, and SMD on the SAMPL1 test set for the prediction of small-molecule solvation free energies. J Phys Chem 113:4538–4543
51. Carpenter JE, Weinhold F (1988) Analysis of the geometry of the hydroxymethyl radical by the "different hybrids for different spins" natural bond orbital procedure. J Mol Struct THEOCHEM 169:41–62
52. Glendening ED, Badenhoop JK, Reed AE, Carpenter JE, Bohmann JA, Morales CM, Weinhold F (2009) NBO 5.9. Theoretical Chemistry Institute, University of Wisconsin, Madison
53. Galano A, Marquez MF, Perez-Gonzalez A (2014) Ellagic acid: an unusually versatile protector against oxidative stress. Chem Res Toxicol 27:904–918
54. Galano A, Alvarez-Idaboy JR (2013) A computational methodology for accurate predictions of rate constants in solution: application to the assessment of primary antioxidant activity. J Comp Chem 34:2430–2445
55. Duncan WT, Bell RL, Truong TN (1998) TheRate: program for ab initio direct dynamics calculations of thermal and vibrational-state-selected rate constants. J Comp Chem 19:1039–1052
56. Marcus RA (1964) Chemical and electrochemical electron-transfer theory. Ann Rev Phys Chem 15:155–196
57. Tiziana M, Galano A, Russo N (2014) Radical scavenging ability of gallic acid toward OH and OOH radicals. Reaction mechanism and rate constants from the density functional theory. J Phys Chem B 118(35):10380–10389
58. Inagaki T, Yamamoto T (2014) Critical role of deep hydrogen tunneling to accelerate the antioxidant reaction of ubiquinol and vitamin E. J Phys Chem B 118(4):937–950
59. Tejero I, González-García N, González-Lafont A, Lluch JM (2007) Tunneling in green tea: understanding the antioxidant activity of catechol-containing compounds. A variational transition-state theory study. J Am Chem Soc 129(18):5846–5854
60. Chiodo SG, Leopoldini M, Russo N, Toscano M (2010) The inactivation of lipid peroxide radical by quercetin. A theoretical insight. Phys Chem Chem Phys 12(27):7662–7670
61. Leopoldini M, Chiodo SG, Russo N, Toscano M (2011) Detailed investigation of the OH radical quenching by natural antioxidant caffeic acid studied by quantum mechanical models. J Chem Theory Comput 7(12):4218–4233
62. Huguenin J, Ould Saad Hamady S, Bourson P (2015) Monitoring deprotonation of gallic acid by Raman spectroscopy. J Raman Spectrosc 46(11):1062–1066
63. Galano A, Alvarez-Idaboy JR (2013) A computational methodology for accurate predictions of rate constants in solution: application to the assessment of primary antioxidant activity. J Comput Chem 34(28):2430–2445
64. Mayer JM, Hrovat DA, Thomas JL, Borden WT (2002) Proton-coupled electron transfer versus hydrogen atom transfer in benzyl/toluene, methoxyl/methanol, and phenoxyl/phenol self-exchange reactions. J Am Chem Soc 124:11142–11147
65. Martínez A, Galano A, Vargas R (2011) Free radical scavenger properties of á-mangostin: thermodynamics and kinetics of HAT and RAF mechanisms. J Phys Chem B 115(43):12591–12598